A THERMAL MODEL STUDY OF A HYPOTHETICAL FRACTURED OIL RESERVOIR

By

JAMES ROBERT CLARK

Bachelor of Science

Oklahoma State University

Stillwater, Oklahoma

1962

Submitted to the faculty of the Graduate School of
the Oklahoma State University
in partial fulfillment of the requirements
for the degree of
MASTER OF SCIENCE
May, 1964

OKLAHOMA
STATE UNIVERSITY
LIBRARY
JAN 8 1965

A THERMAL MODEL STUDY OF A HYPOTHETICAL

FRACTURED OIL RESERVOIR

Thesis Approved:

Thesis Adviser

Dean of the Graduate School

570169

ACKNOWLEDGEMENTS

I would like to express my sincere appreciation to the following individuals for their assistance in making this thesis possible:

To L. D. Bachman, E. W. Adams, W. S. Foster and E. L. Dowty for their advice and physical aid during the experimental portion of this study.

To O. J. Burchett for his assistance with the photography.

To my parents and parents-in-law for their encouragement during my graduate study.

To my wife, Gayle, for her patience and direct assistance during the past year.

To Mrs. Mildred Avery for her guidance and help during my attendance at Oklahoma State University.

To Professor A. G. Comer for the important part he played in my graduate training, and also for his advice during the research investigation.

To Mrs. R. M. Schenandoah for typing this thesis.

In addition, deep gratitude is expressed to the Pan American Oil Corporation for the fellowship which made my graduate schooling and research possible.

TABLE OF CONTENTS

LIST OF TABLES

LIST OF FIGURES

CHAPTER I

INTRODUCTION

Since about 1948, formation fracturing has become an important part of the oil industry. In many cases this operation has been extremely profitable due to increases in productivity and ultimate oil recovery. There have been numerous studies made to predict the effects of formation fracturing in order to determine whether or not this operation would be feasible.

Formation fracturing as used here refers to the splitting of reservoir rock in order to increase its average permeability. Hydraulic pressure is applied to the zone to be fractured, and when the applied pressure exceeds the stresses existing in the rock, a split is initiated. The fracture discussed in this study is a horizontal circular, or "pancake" fracture.

It has been found possible to reasonably predict reservoir behavior through the use of model studies. Scaled fluid models have been used; and where proper analogies have been made, electrical and thermal models have yielded valid information. The subject of this research investigation includes the use of thermal models to simulate a hypothetical reservoir which in two instances was fractured, and in one instance was not. All reservoir characteristics were the same for the fractured models, except that one allowed fluid entry to the well along the entire length of the wellbore, while the other was restricted to entry only at the point of intersection of the fracture and the wellbore.

The assumption of point entry is often quite logical due to the fact that wellbore damage is in many cases the reason for fracturing. Once the "skin" of reduced permeability is pierced, a large percent of the production will be through the rupture. In other instances, wellbore damage may not be serious and fluid will be produced along the total length of the wellbore. A comparison has been made here to determine which type of entry is more effective in depleting an oil reservoir. In addition, the behavior of the fractured reservoir is compared with that of an identical, but unfractured, reservoir.

CHAPTER II

PREVIOUS INVESTIGATION

Fracturing changes the average permeability of an oil reservoir and thus changes the flow characteristics. The inhomogeneity introduced makes analytical descriptions difficult and incurs the use of various simplifying assumptions. The following lists some of the these assumptions:

(1) The flow into the wellbore is only through the fracture.

(2) The reservoir is horizontal, homogeneous, isotropic and has uniform thickness.

(3) The fracture is of uniform flow capacity and is radial.

(4) A single fracture exists.

(5) After sufficient production time, the system is in a steady state of flow with a radial drainage boundary.

The skin effect has been used to study the behavior of fractured reservoirs. Skin effect may be defined as pressure drop, between the drainage and wellbore radii, caused by the presence of an altered zone (or skin) of reduced permeability.

Hartsock and Warren (1)[1] have stated that the productivity of a hydraulically fractured system relative to that of an unfractured well, can

---

[1]Note: ( ) refers to Selected Bibliography.

be determined from the apparent skin effect and can be used to establish design objectives. They further state that both the radius and flow capacity of a fracture cannot be uniquely determined from the apparent skin effect; an independent determination of one of the quantities is necessary.

Their apparent skin effect is given by:

$$S = \frac{2\pi(kh)_r}{q\mu B_o}\left[(\Delta P)_f - (\Delta P)_r\right] \qquad (2\text{-}1)$$

For evaluating a fracture treatment, the skin effect can be found by two methods. When a pressure build-up test is run after a well has been fractured, if an adequate linear segment is obtained when the shut-in pressure is plotted versus log $(t+\Delta t)/t$; the skin effect can be calculated from:

$$S = 1.15\left(\frac{P_{wi}-P_{wo}}{m} - \log_{10}\frac{B_o q}{m\phi\, chr_w^2} + 1\right) \qquad (2\text{-}2)$$

If stabilized productivity indices are measured just before fracturing, $(PI)_r$, and immediately after fracturing, $(PI)_f$, the skin effect can be determined from:

$$S = (\ln {}^{re}/_{rw} - .75)\left[1 - \frac{(PI)_r}{(PI)_f}\right] \qquad (2\text{-}3)$$

For identical drawdowns, the ratio of productivity indices can be replaced by the ratio of the production rates, q_r/q_f.

Generally, for a fixed pressure drawdown and a fixed average reservoir pressure,

$$q_f = \left(\frac{\ln {}^{re}/_{rw} - .75}{\ln {}^{re}/_{rw} - .75+S}\right) q_r \qquad (2\text{-}4)$$

To evaluate a fracture treatment, the apparent skin effect can be calculated from Equation (2-2) or Equation (2-3), and this value can be used with Equation (2-4) to find q_f/q_r.

In addition to the previously mentioned assumptions, this method also assumes that fluid is flowing from the reservoir to the well at a constant rate; and that the apparent skin effect, due to the distortion of the flow pattern by the fracture, can be calculated from an assumed steady state pressure distribution. This distribution exists between the well and the "critical radius." The critical radius is the distance from the well at which flow is purely radial and at which a cylindrical surface of constant pressure is present.

According to Dr. H. K. Van Poolen (2), increased well productivity can be obtained by fractures opening up a flow channel through the damaged zone around the wellbore. Mathematical analyses of electrical models have shown this increased productivity and have also shown the following: larger fractures mean greater productivity increase; increase of fracture flow capacity results in greater production potential; damage to the formation immediately surrounding a fracture has little effect on well productivity, while damage to fracture flow capacity has a major effect; most production will enter the fracture in that portion of the fracture farthest away from the wellbore.

In all the cases discussed by Dr. Van Poolen, the following assumptions were made: The formation is homogenous and isotropic (constant permeability, constant porosity); the fluids are incompressible and homogeneous; the system is in a steady state of flow; and the effect of gravity is ignored.

Crawford and Landrum (3) have made similar studies of electrical models with simulated horizontal fractures. Their data applies to uniform and homogeneous reservoirs which are producing at steady state conditions. They indicate that the creation of a single large pancake fracture will possibly be more effective in obtaining a large increase in the production capacity of the well than the creation of several fractures of small radius. It was also found that the inclination of a circular fracture from horizontal results in a decrease of production capacity of the well, and that the effect of an elliptical fracture on production capacity appears very similar to the effect of a circular fracture whose radius is equal to the arithmetic average radius of the ellipse.

A heat conduction model has been used (4) to study the flow of fluids in a stratified oil reservoir which is being subjected to unsteady state depletion. To simulate stratification, plates of different metals were joined together so that cross flow could occur between strata. It was concluded that a layered reservoir with cross flow can be considered as a uniform homogeneous reservoir of the same thickness and length if the permeability-porosity ratio is represented by $(\Sigma kh/\Sigma \phi h)$. It was emphasized that this recommendation applies when the reservoir approaches pseudo-steady state because the effective value of k is larger during the earlier transient period.

This model has shown the applicability of the thermal analogy to fluid flow. It is quite important that reservoir inhomogeneities can be approximated by a thermal model and that the reservoir can be considered as a homogeneous one if the proper permeability-porosity ratio is computed.

Another heat conduction model (5) has been developed to predict the pressure distribution within a reservoir being subjected to unsteady state depletion. An analogy between the flow of fluid in an unsymmetrical reservoir and conduction of heat in a similarly shaped unsymmetrical metal plate was made to show adaptability of the heat conduction principle to transient reservoir cases.

CHAPTER III

STATEMENT OF PROBLEM

Literature is filled with solutions to problems pertaining to homogeneous oil reservoirs of simple geometry. Steady state conditions greatly simplify the mathematics used in analytical studies, and these conditions are readily simulated by potentiometric models.

On the other hand, transient fluid flow is quite difficult to describe analytically and studies of its behavior require various assumptions and approximations. Description of this type of flow is made even more difficult when the transmitting medium is of irregular geometry and is heterogeneous and anisotropic.

The transient nature of heat flow is very similar to the transient behavior of single-phase fluid flow and this fact suggests the use of a thermal model to analyze unsteady state behavior of an inhomogeneous reservoir.

Stimulation techniques, such as hydraulic fracturing, introduce variations of reservoir properties and of fluid flow behavior. Thus, the problem is to analyze the possiblity of using a thermal model to study the transient behavior of a fractured oil reservoir, producing above the bubble point by liquid expansion drive; and to check the validity of the assumption of point entry of fluid into the wellbore of a fractured formation.

CHAPTER IV

EXPERIMENTAL EQUIPMENT AND PROCEDURE

One of the model reservoirs used in this study is shown in Figure 1, with an accompanying illustration in Figure 2. It was made of United States Gypsum's Number One moulding plaster, and the well was represented by a 1/4-inch copper tube. The fracture was made of a 0.0031-inch thick copper sheet. Two of the models studied contained fractures while the third did not.

The models were used to approximate sections of radial reservoirs, and the copper sheets were used to simulate sections of horizontal radial fractures. The fractures were placed at the vertical center of the model and were bonded to the wellbore by means of a tab of copper which was left at the tip of the fracture when it was cut. The tab was wrapped around the copper wellbore, then soldered. This assured good contact and also helped to hold the fracture in place while the model was being poured.

Forms for the model were made of 1/2-inch plywood. Experience showed that the plaster, upon drying, adhered to the wood, resulting in the formation of cracks and voids in the model. Application of diesel oil to the inside of the forms did not solve this problem, but it was found that lining the forms with aluminum foil did solve it, and also permitted the reuse of the same form several times.

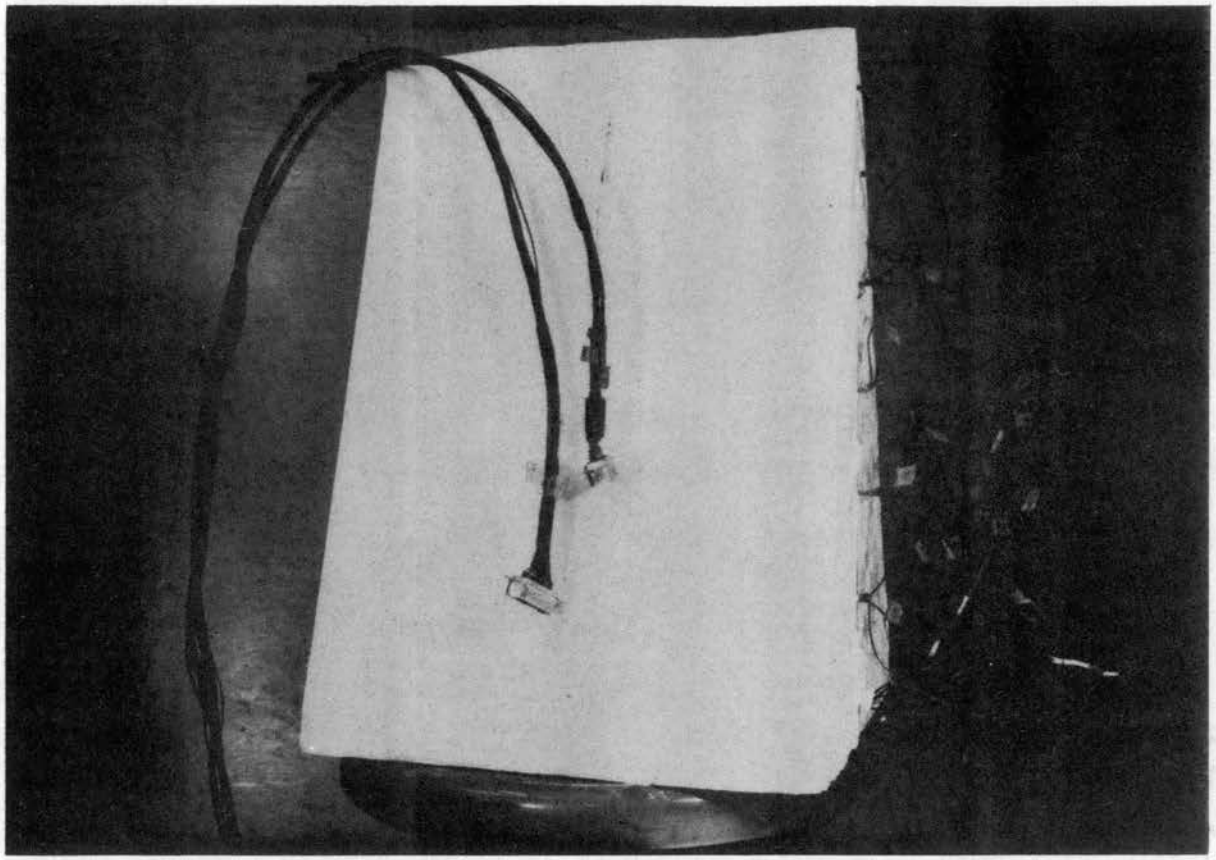

Figure 1. Uninsulated Model Reservoir

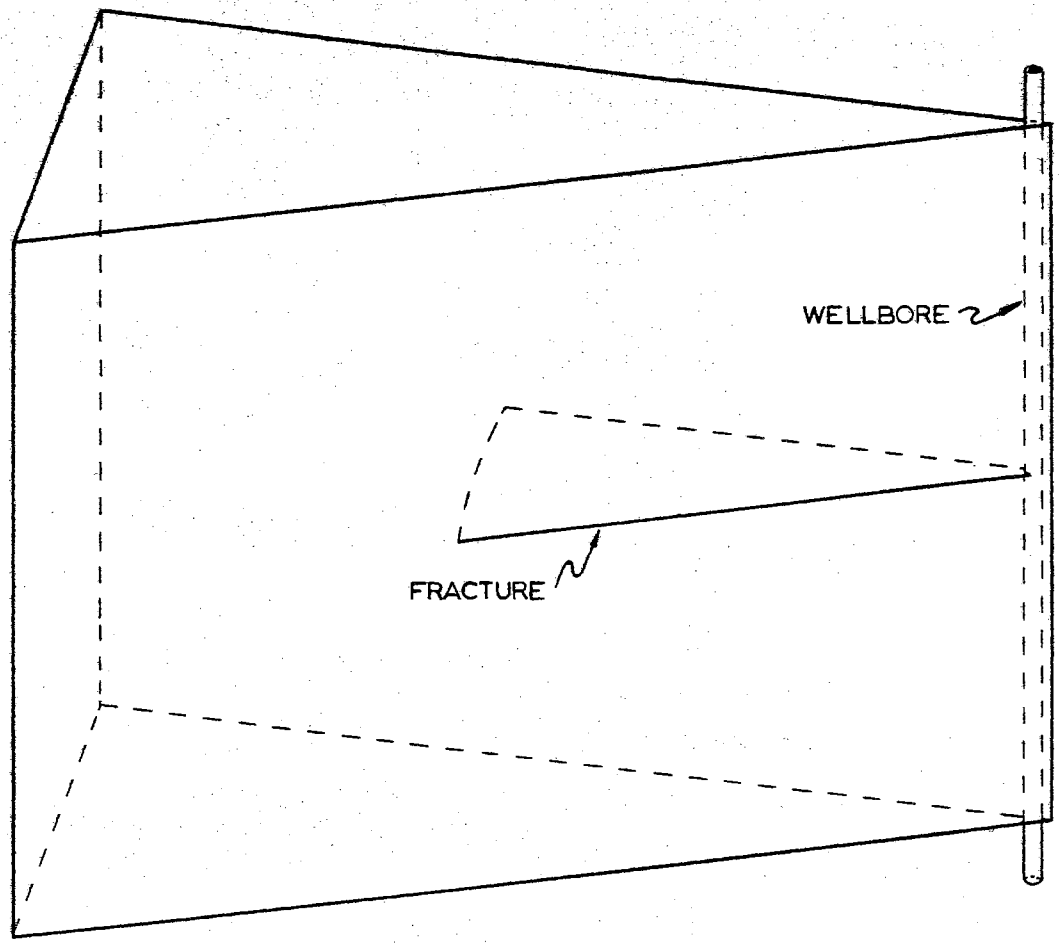

Figure 2. Fractured Model with Total Wellbore Entry.

The fracture was held in place during pouring by making it too wide in the angular direction, folding the excess to form a right angle with the fracture, and then taping and stapling the excessive copper to the sides of the form. When the form was removed, this excess copper was exposed and was trimmed from the model.

Thermocouples were located in the model as shown in Figure 3. A problem existed in properly locating the thermocouples and holding them in position as the plaster was being poured. Since there was to be vertical alignment, rigid columns consisting of three thermocouples each were formed by twisting the thermocouple wires together and wrapping them with thread. Each column was then inserted into a properly spaced notch on a strip of plywood so that the bottom thermocouple of the column would hang the proper depth into the form when the jig was nailed along the center line of the top of the form. The columns were then anchored in place by attaching a length of thread to each of the bottom thermocouples. The other end of the threads were passed through tiny holes which had been drilled at proper intervals in the fracture and in the bottom of the form. Tension was then applied to the threads and they were tied to thumbtacks on the bottom of the form. The holes in the copper prevented the fracture from bowing up during the pouring of the plaster, and also prevented trapping of air beneath the fracture.

Tests were performed with small quantities of the moulding plaster to determine what proportion of water to plaster would yield the best moulding mixture. It was decided that one quart of water to each 3.57 pounds of plaster formed the desired mixture. Care was taken to prepare a sufficient amount of plaster to make a complete pour. When fresh plaster was

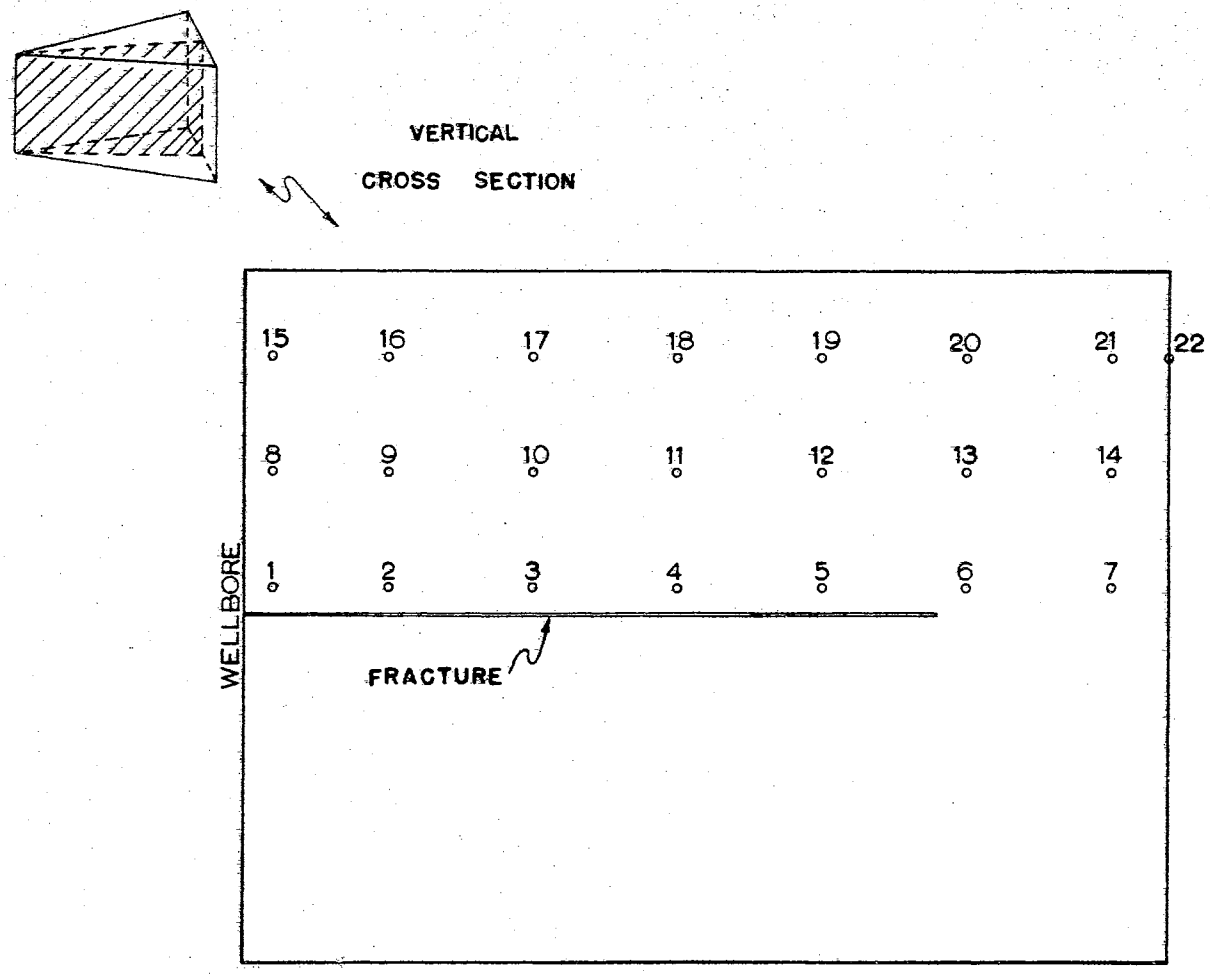

Figure 3. Model Cross Section Showing Thermocouples.

poured onto partially set plaster, a cleavage plane was formed and the model separated upon heating. Tapping of the form during pouring insured filling of all parts of the form and thus prevented large voids from being formed due to trapped air. Speed was required in mixing and pouring the plaster, in that it was observed that the mixture would set up in about five minutes after the addition of water.

The thermocouples used were made of 30-gauge iron-constantan wire. For quick and easy connection, two pairs of 24-contact male and female connector plugs were used. The two female plugs were permanently attached to a recorder and the two male plugs were attached to the model. The thermocouple wires were made long enough initially to allow them to be cut off at the model and rewelded into new thermocouples, thus saving the tedious job of soldering new wires to the male plugs each time a new model was made.

The thermocouple wires were taped together after being soldered to the plug. This prevented not only tangling, but also breaking of the wires. The individual wires were labeled at both ends and their identities were reestablished, with the aid of an ohmeter, each time they were trimmed from a model.

The models were completely covered with four layers of 3/8-inch Cerafelt insulation. The insulation was attached with Elmer's Glue, which was found sufficient in the temperature range used. A powdered fibrous insulation was mixed with water to form a paste which was used to seal the joints formed by the Cerafelt and which was also used to mould around the wellbore where the tube protruded from the model.

Symbols used in Table I:

$A = m_{NiSO_4}$

$B = 4m_{NiSO_4}$

$C = -\log 4m_{NiSO_4}$

$D = -k \log 4m_{NiSO_4}$

$E = E^o - k \log 4m_{NiSO_4}$

$F = k \log \frac{\gamma^2_{\pm NiSO_4}}{\gamma^3_{\pm NiCl_2}}$

$G = \log \frac{\gamma^2_{\pm NiSO_4}}{\gamma^3_{\pm NiCl_2}}$

$H = \frac{\gamma^3_{\pm NiCl_2}}{\gamma^2_{\pm NiSO_4}}$

$I = \frac{1}{m_{Ni^{++}}}$

$J = \log \frac{1}{m_{Ni^{++}}}$

$K = \left(\frac{\Delta E}{\Delta T}\right) = \text{slope} \times 10^4$

minutes of the run. Apparently this difference had neglibible effects on the cooling of the models. A check thermocouple was placed in the bottom half of each of the models, symmetrically located with respect to one of the thermocouples in the upper half. The temperatures recorded by the check thermocouple were noted to be identical with those recorded by its corresponding thermocouple. This also indicated that symmetry did exist in the vertical direction, and that the models were physically homogeneous.

The temperature of the coolant was found to vary somewhat with flow rate, therefore the flow rate was monitored. The flow rate was measured with a stopwatch and a graduated cylinder. For all three runs the rate of flow was held at 100 cc in 50 seconds. Given weights of outlet water were caught during measured time periods in hopes that the difference in inlet and outlet temperatures could be used to calculate the thermal energy dissipated in the coolant. This calculation could not be made due to the small temperature rise and the large range of the recorder.

The hypothetical reservoir which the thermal models represented had the following characteristics:

Shape - approximately radial

Radial length - 3000 ft.

Thickness - 10 ft

Permeability - 2.25 md

Porosity - 25 percent

Liquid viscosity - 1 cp

Liquid compressibility - 6×10^{-5} atm^{-1}

and for the fractured reservoirs:

Fracture radius = 2,250 ft

Fracture thickness = .031 in

The following assumptions were made:

1. The fluid fully saturated the reservoir, and was produced above the bubble point,
2. The reservoir was horizontal, and gravity effects were negligible.
3. Vertical and horizontal formation permeability were equal,
4. The reservoir was homogeneous and isotropic except for the fracture.
5. The exterior boundary of the reservoir in the radial direction was impermeable to flow.

The model and associated apparatus are shown in Figure 4. The model reservoir had the following characteristics:

Shape - as shown in Figure 2

Radial length - approximately 12 in

Thickness - 12 in

Thermal diffusivity - 0.0029 cm^2/sec

and in addition, for the fractured models:

Fracture radius - 9 in

Fracture thickness - 0.0031 in

A correlation between fluid flow in a porous material and heat conduction through a solid can be found in Appendix A. The equations presented will be used in making analogies between the theoretical reservoir and and the thermal models.

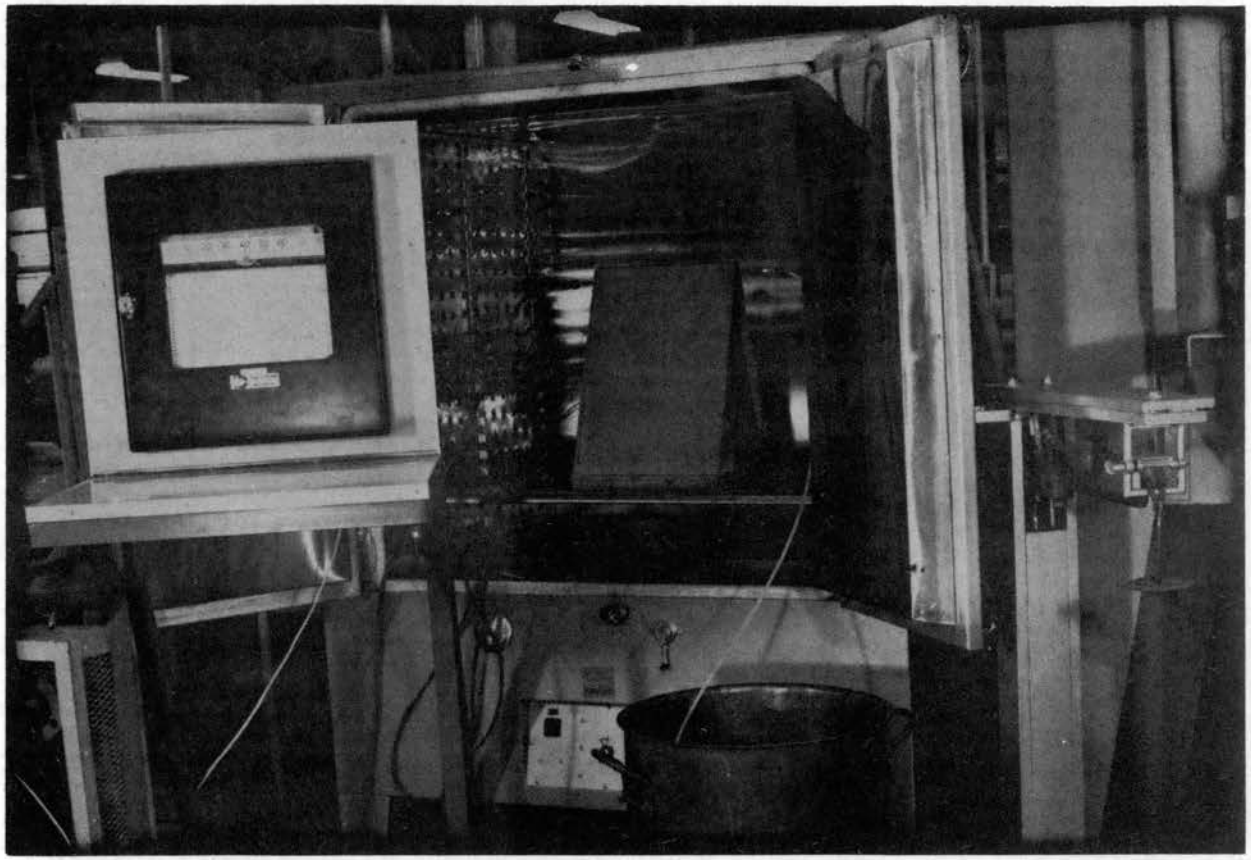

Figure 4. Model and Associated Apparatus

Pressure and temperature were the driving potentials in the reservoir and model, respectively. When both were put into dimensionless form and equated, the result was:

$$\frac{P_i - P}{P_i - P_w} = \frac{T_i - T}{T_i - T_w} \tag{4-1}$$

The initial reservoir pressure was chosen as 2000 psi, and the constant wellbore pressure was chosen as 1700 psi because these values best illustrated the difference in behavior of the reservoirs. All three models were heated to an initial temperature of 400° F, and the temperature at the well was held at about 92° F. The recorded model temperatures were converted to reservoir pressures by the expression:

$$P = P_i - \left(\frac{T_i - T}{T_i - T_w} \right) (P_i - P_w) \tag{4-2}$$

As previously mentioned, the wellbore temperature, T_w, varied slightly. Proper values of T_w were used in Equation (4-2) at the various times that were considered.

In order to correlate reservoir time with model time, both were made into dimensionless times and equated. After solving for the reservoir time:

$$t_r = \alpha \frac{\mu}{k} \frac{L_r^2}{L_m^2} \phi c \, t_m \tag{4-3}$$

Substitution of the previously mentioned values into this equation gave:

$$t_r = 180 \, t_m \tag{4-4}$$

This meant that each hour of model time was the equivalent of 180 hours of reservoir time.

Each of the runs lasted 18 hours and 20 minutes, model time; or 3300 hours, reservoir time. This allowed the pressures to drop from 2000 psi to approximately 1740 psi. It should be realized that if the runs had lasted long enough, the whole reservoir would have reached the wellbore pressure.

Advantages were taken of the symmetry of the radial reservoir. Symmetry existed in both the vertical and angular directions. This allowed the thermocouples to be located in the top half of the model only, and also made it possible to use only a section of the reservoir to describe its entirety. The horizontal cross section of the model was simply one section of a 12-sided polygon. For purposes of comparison between the three models, the polygon section was assured to be a circular sector. The difference in cross sectional areas was found to be:

For the circle sector,

$$A = \pi r^2 \frac{\theta}{360}$$

$$A = 37.8 \text{ in}^2$$

For the polygon section,

$$A = 1/2 \text{ base} \times \text{height}$$

$$A = 38.6 \text{ in}^2$$

The models were made in the polygonal shape because of the ease of moulding.

The moulded plaster was found to decrease in density when heated for the first time, so the models were baked for several hours before being insulated. This drying process prevented changes in thermal properties during the runs, and also prevented shrinkage cracks when the temperature was raised to 400° F.

At least 48 hours were required to heat the entire model to 400° F. One side was left uninsulated until this temperature was attained, then the side was quickly insulated and further heating was applied to assure constant temperatures throughout the model.

After a run was completed, the temperatures were plotted versus time in order to check for any obvious errors. From these graphs was obtained information with which to make plots of temperature versus distance, at a given time. If no gross discrepancies appeared in these curves, then the model was broken up. The broken model was thoroughly examined in search of air pockets or other undesirable conditions. At this time it was noted that the method used to position the thermocouples had been successful.

Samples were taken from the top, middle, and bottom of the model and the densities were measured with a pycnometer. The results showed that each model was homogeneous in density and that the three models were approximately equal in density. The density was used with Figure 5 to determine the thermal conductivity of the models. The dry density was found to be 62.1 lb/ft^3 which corresponded to a thermal conductivity of 2.25 Btu. in/hr. ft^2° F. The specific heat of the plaster was given as 0.26 Btu/lb.° F, and the thermal diffusivity was calculated to be 0.00299 cm^2/sec, from the equation:

$$\alpha = (0.0215)\ \frac{K}{\rho C} \qquad (4\text{-}5)$$

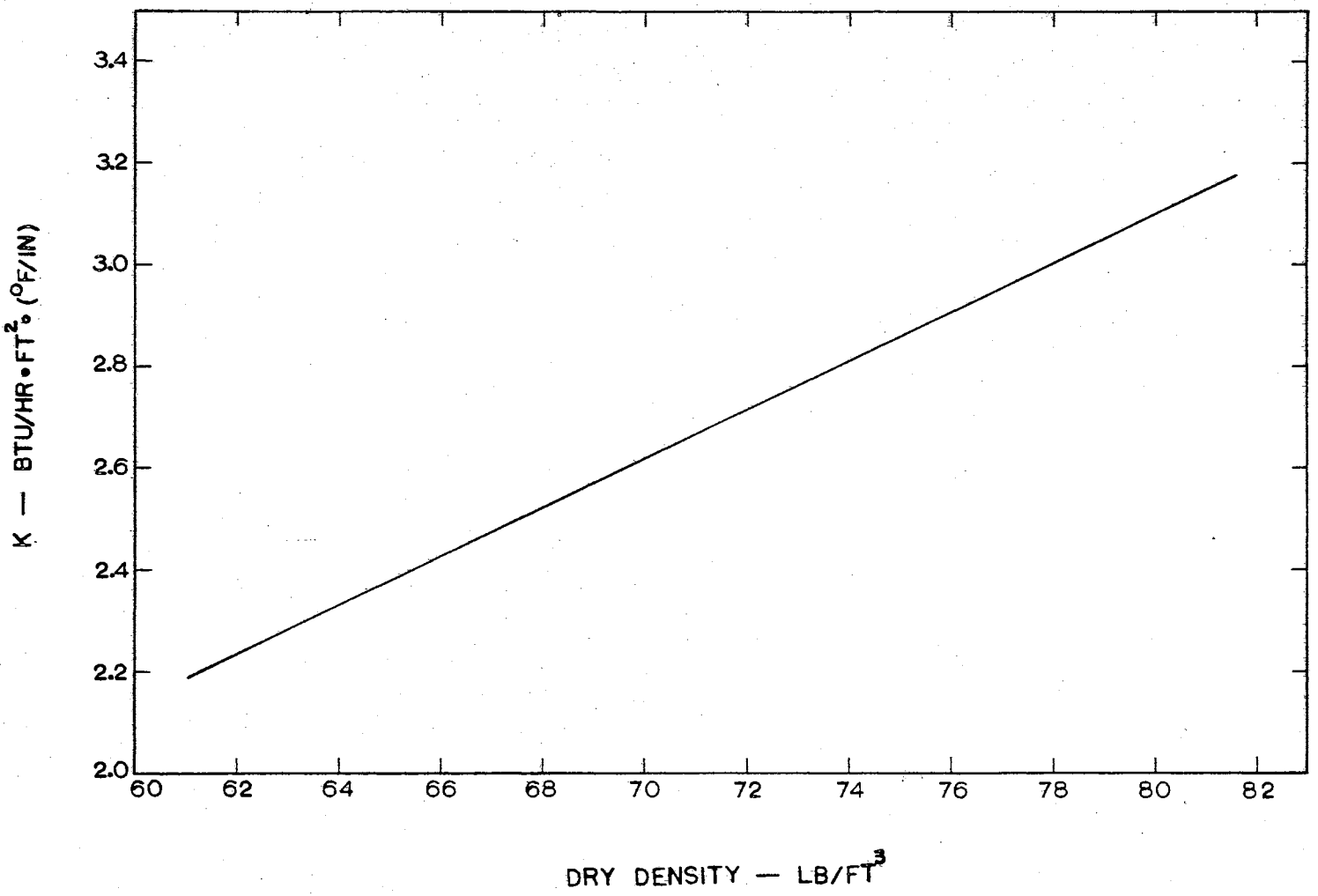

Figure 5. Thermal Conductivity Versus Dry Density for the Moulding Plaster.

As for scaling of distance, it was found that 1 model inch in the radial direction represented 250 reservoir feet, while 1 model inch in the vertical direction represented 0.834 reservoir feet. This information, along with the various temperature, distance and time graphs allowed examination of the behavior of the theoretical oil reservoir.

The temperatures and model times were changed to pressures and reservoir times by the use of Equations (4-2) and (4-4), respectively. Model locations were converted to reservoir locations by using the previously mentioned scale factors, and plots were made of (a) pressure versus time, at a given location; (b) pressure versus radial distance, at given times and heights, and (c) constant pressure lines at given times for vertical cross sections of the models.

From part (c) of the preceding paragraph were obtained the average pressures for several given times. Isobars were plotted on scaled vertical cross sections of the reservoirs, and the average pressures were given by:

$$P_{avg} = \frac{\int P \, dA}{A_{(total)}} \approx \frac{\Sigma (P_j A_j)}{\Sigma A_j} \qquad (4\text{-}6)$$

The P_j were taken as the average pressures between isobars, and the A_j were found by planimetering the areas between the isobars.

For an unsteady state compressible liquid reservoir, the amount of fluid which has been removed to develop the pressure distribution at any time and corresponding drainage radius is proportional to (a) the liquid compressibility; (b) the volume of fluid contained in the drainage area, and (c) the drop in average pressure. Therefore, the cumulative volumes

of fluid produced from the reservoirs were determined from the equation:

$$N_p = cV\,\Delta P \tag{4-7}$$

Which may also be written as:

$$N_p = c\left(\frac{\pi L_r^2\, h_r\, \Phi}{5.615}\right)(P_i - P_{avg}) \tag{4-8}$$

where N_p is given in reservoir barrels.

CHAPTER V

EXPERIMENTAL RESULTS

The three models used in this study were to represent the same theoretical reservoir. One model was unfractured and the second contained a horizontal circular fracture at the center of the formation with fluid entry along the entire wellbore. The third was identical to the second, except that fluid entry to the wellbore was allowed only at the intersection of the fracture with the wellbore. This "point entry" of fluid was attained by rotating the copper wellbore 90° from its original position, allowing it to touch the model at the tip of the fracture sector only.

Since all conditions, except the ones mentioned in the preceding paragraph, were duplicated for the three models, any differences in the behavior of the models were attributed to these purposely altered conditions.

Numerous curves were plotted in order to completely examine the information presented by the behavior of the models. Figure 6, for instance, shows pressure decline curves for two different points in the reservoir. Both points are 0.417 ft above (or below) the fracture; one being 125 ft, and the other 1500 ft from the wellbore. These points correspond to thermocouples 1 and 4, respectively, of Figure 3. Similar curves were plotted for reservoir locations corresponding to all of the thermocouple positions in the models.

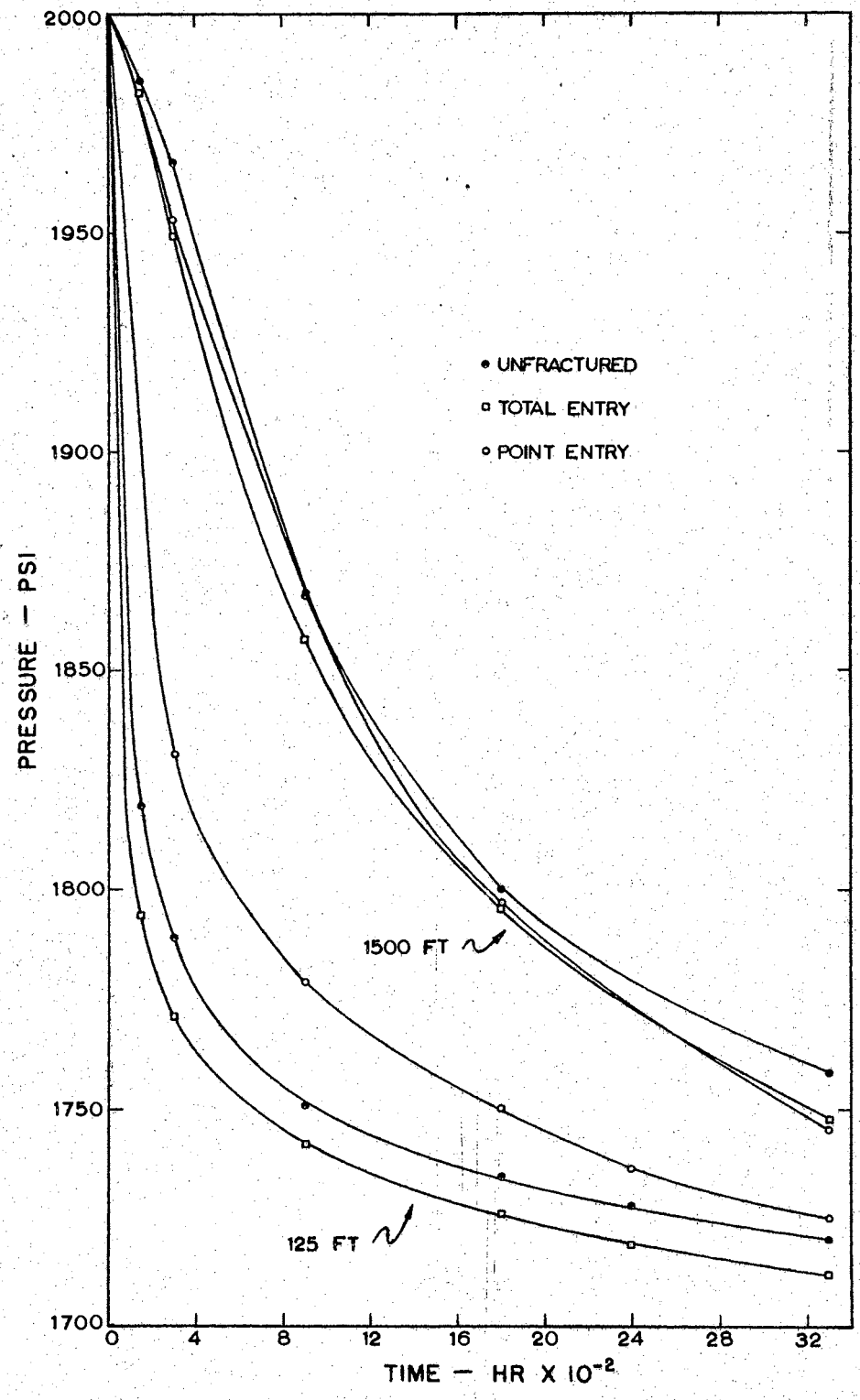

Figure 6. Pressure Decline for Points 1 and 4 of Figure 3.

Figure 6 shows that the pressure at any given time was lower for the total-entry fractured model than for the unfractured one. This was also found to be true at all the other reservoirs locations which were examined. The point-entry model at 125 ft was found to have higher pressures than the other models; but at greater distances from the wellbore the comparative pressures were more like that of the 1500 ft curves of Figure 6.

From the pressure versus time graphs were obtained curves such as those of Figures 7 and 8. These figures show how the pressure varied with radius for given reservoir times.

Figure 7 shows plots of pressure versus radius for the total-entry fractured reservoir and the unfractured reservoir at a vertical distance of 0.417 ft from their centers; while Figure 8 shows the same type of plot for the two fractured reservoirs at a vertical location of 2.085 ft from their centers. At 300 hours, which corresponded to 1 hour and 40 minutes of model time, the total-entry fractured reservoir pressures were about 20 psi lower than those of the unfractured reservoir. This pressure difference existed near the well and began to decrease at approximately one-half the radius of the reservoir. The difference at the extreme radius of the reservoir was noted to be only 2 psi. Figure 7 indicates that a pressure difference of about 10 psi existed along the entire radius after 3300 hours of production.

The fractured reservoirs are compared in Figure 8. As was expected, the point-entry reservoir had higher pressures near the wellbore except at the point of contact between the fracture and wellbore. This difference diminished toward the outer edges of the reservoir, and at some of

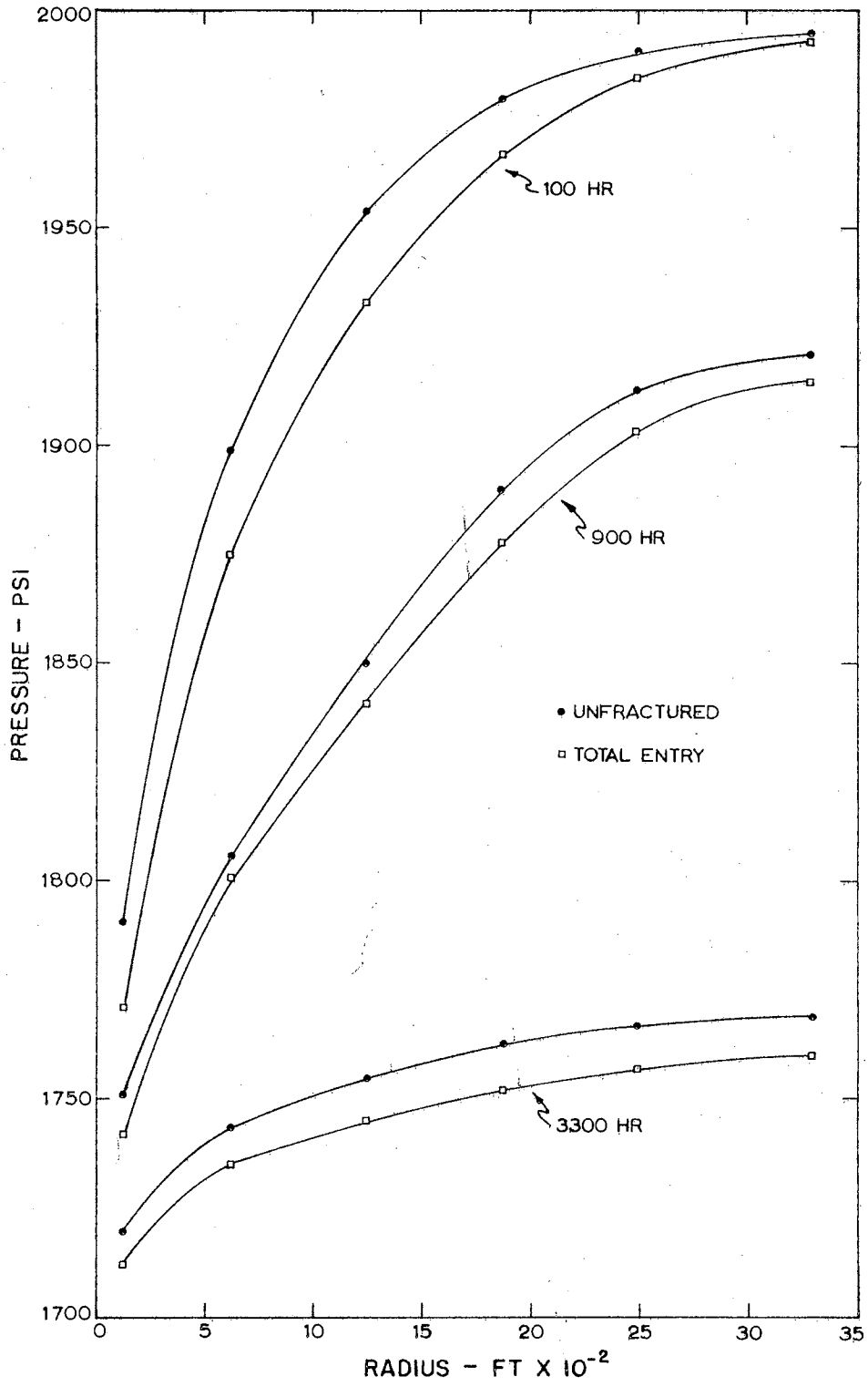

Figure 7. Pressure Versus Radius at .417 Vertical Feet from the Reservoir Center.

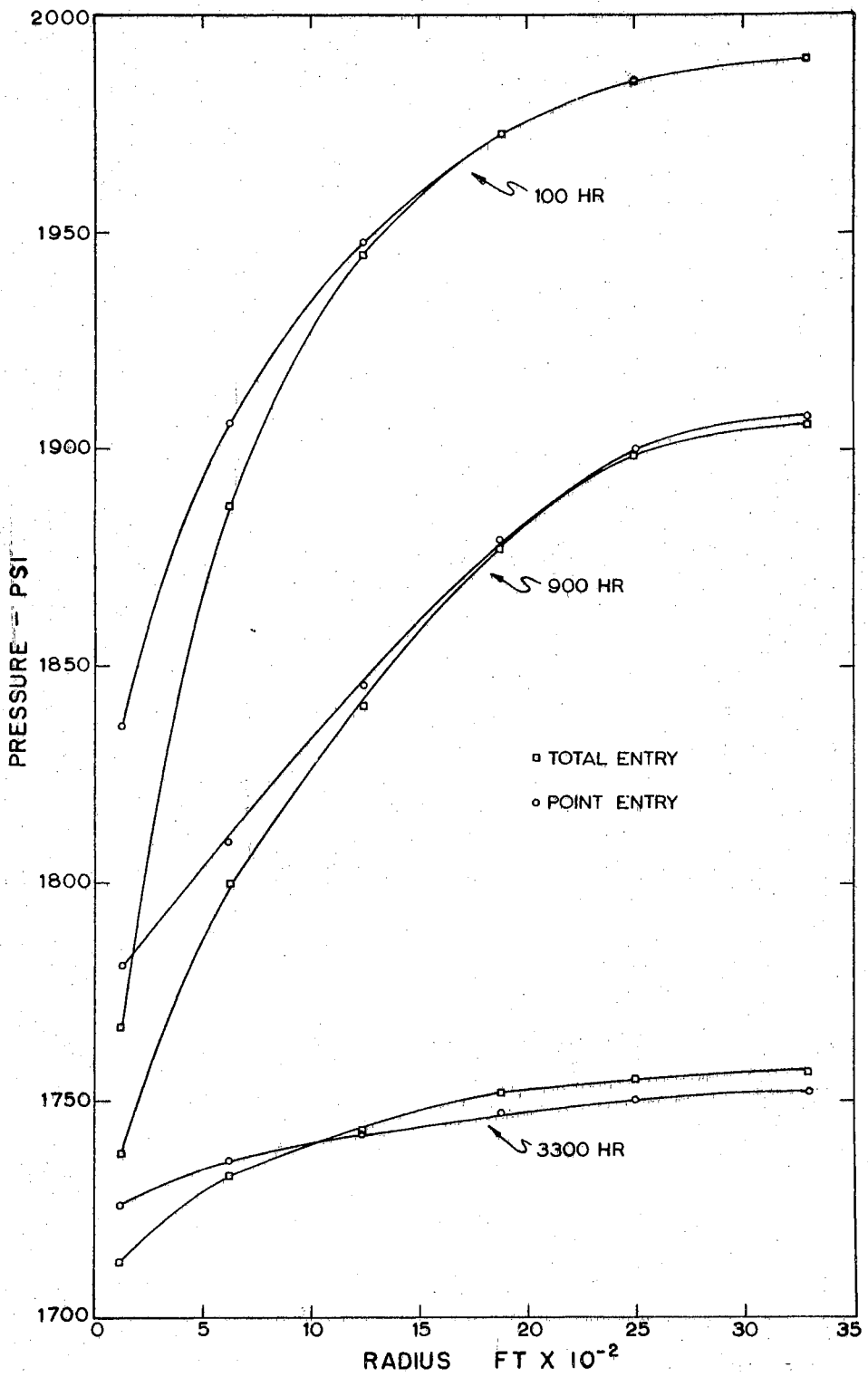

Figure 8. Pressure Versus Radius at 2.08 Vertical Feet from the Reservoir Center.

the outer locations, the point-entry pressures were lower.

The preceding figures gave only an idea of the differences that existed in the three reservoirs. In order to actually compare the performances, the pressure, time and distance data were transformed into production data. The first step was to obtain isobaric maps for various reservoir times. These maps were derived from curves such as those of Figures 7 and 8. A few of the results are shown in Figures 9 and 10.

Figure 9 shows vertical cross sections taken the same as that of Figure 3. These particular pressure profiles were present after 300 hours of production time. Deviation from purely radial flow can be noted from these figures. Similar maps were drawn for 900, 1800, 2400 and 3300 hour reservoir times. Figure 10 contains the maps for 3300 hours.

Each of the areas of the pressure contour maps was determined with a planimeter, then the average reservoir pressures were computed from Equation (4-6). Table I shows the data associated with the unfractured reservoir at 3300 hours.

TABLE I

EXAMPLE CALCULATION OF AVERAGE RESERVOIR PRESSURE

j	P_j(psi)	A_j(in^2)	$(P_j)X(A_j)$
1	1713	1.49	2560
2	1733	3.10	5380
3	1745	3.70	6450
4	1753	3.00	5270
5	1758	4.78	8410
6	1763	5.10	9000
7	1768	3.43	6060
		24.60	43,130

$$P_{avg} = \frac{43,130}{24.60} = 1756 \text{ psi}$$

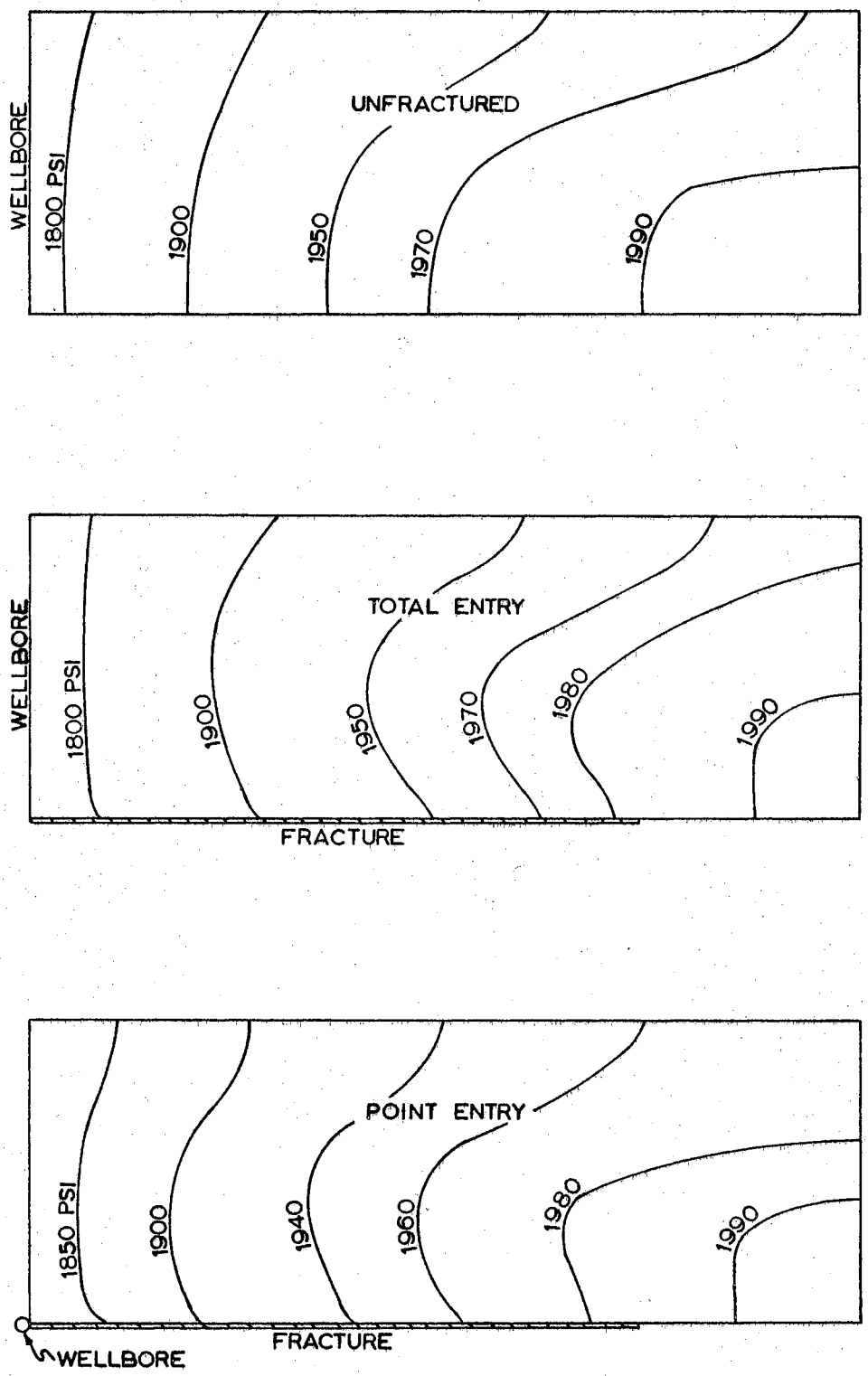

Figure 9. Vertical Cross Sections Showing Isobaric Lines at 300 Hours.

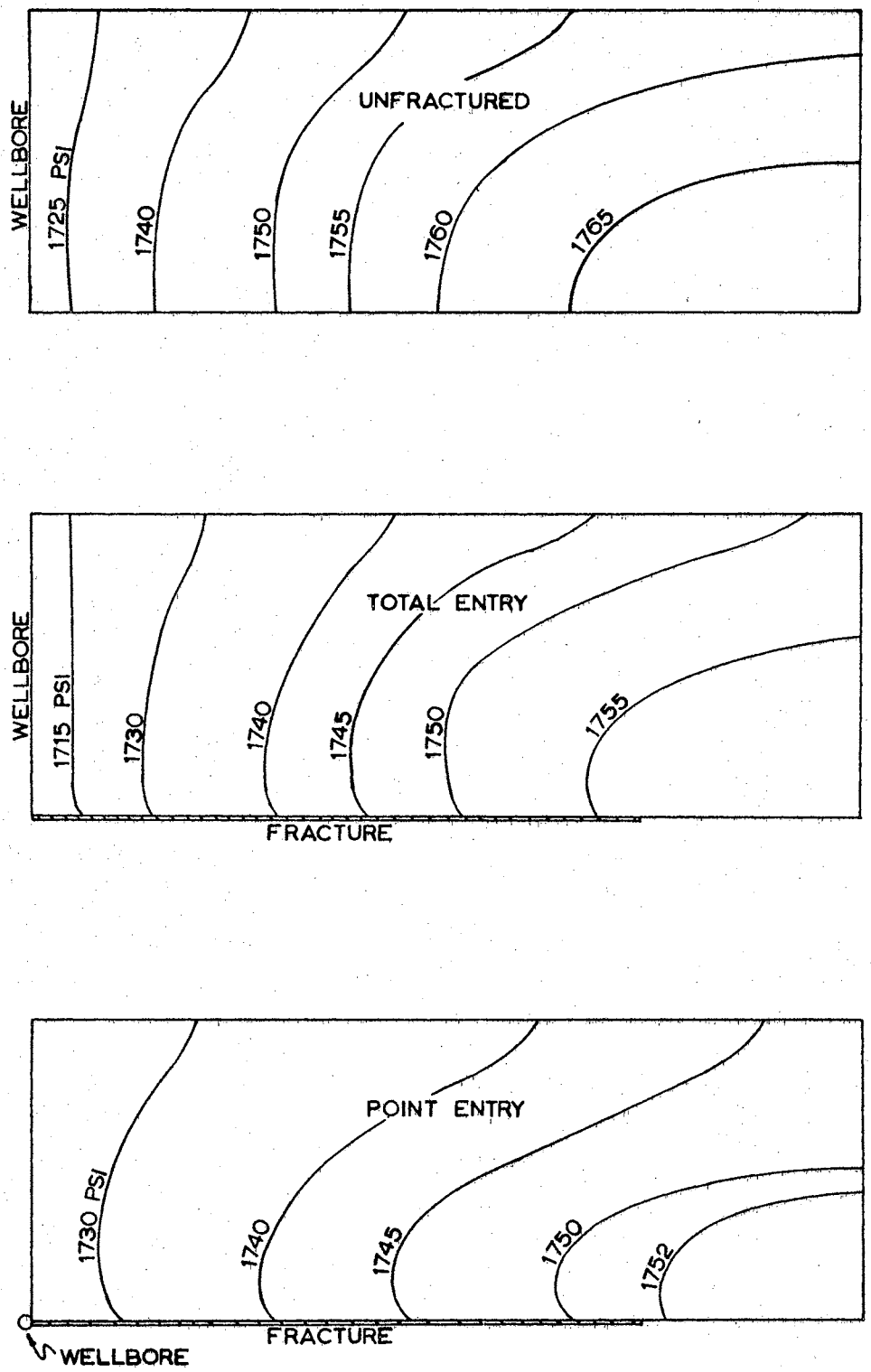

Figure 10. Vertical Cross Sections Showing Isobaric Lines at 3300 Hours.

Similar calculations were performed for all three models and the declines of the average reservoir pressures were plotted as shown in Figure 11. Average pressures for the fractured reservoirs were lower than those of the unfractured one throughout the depletion period studied. The point-entry reservoir pressure is higher than the other fractured reservoir pressure until near the end of the production period, then the two pressures become identical.

The average reservoir pressures were used in conjunction with Equation (4-8) to obtain the cumulative productions for the three cases at any given time. Figure 12 shows the productions for the total-entry fractured reservoir, and also for the unfractured one. As was expected, the fractured reservoir exceeded the unfractured one in production during the considered time period. With no driving mechanism other than liquid expansion, the reservoirs would have eventually assumed average pressures equal to that of the well pressure. The production at that time would have been 226,200 reservoir barrels of oil.

Shown in Figure 13 is a plot of cumulative production versus time for the two fractured cases. Since the production was found by multiplying a constant times the pressure drop, the curves have the same relative shape as the pressure versus time curves. As the difference in reservoir pressures decreased for these two reservoirs, so did the difference in productions.

The results of the tests were as expected, but the magnitude of the difference in behavior of the three reservoirs was not as great as was desired. Although the thermal conductivity of the Cerafelt was 7 1/2 times smaller than that of the plaster, the major reason for lack of

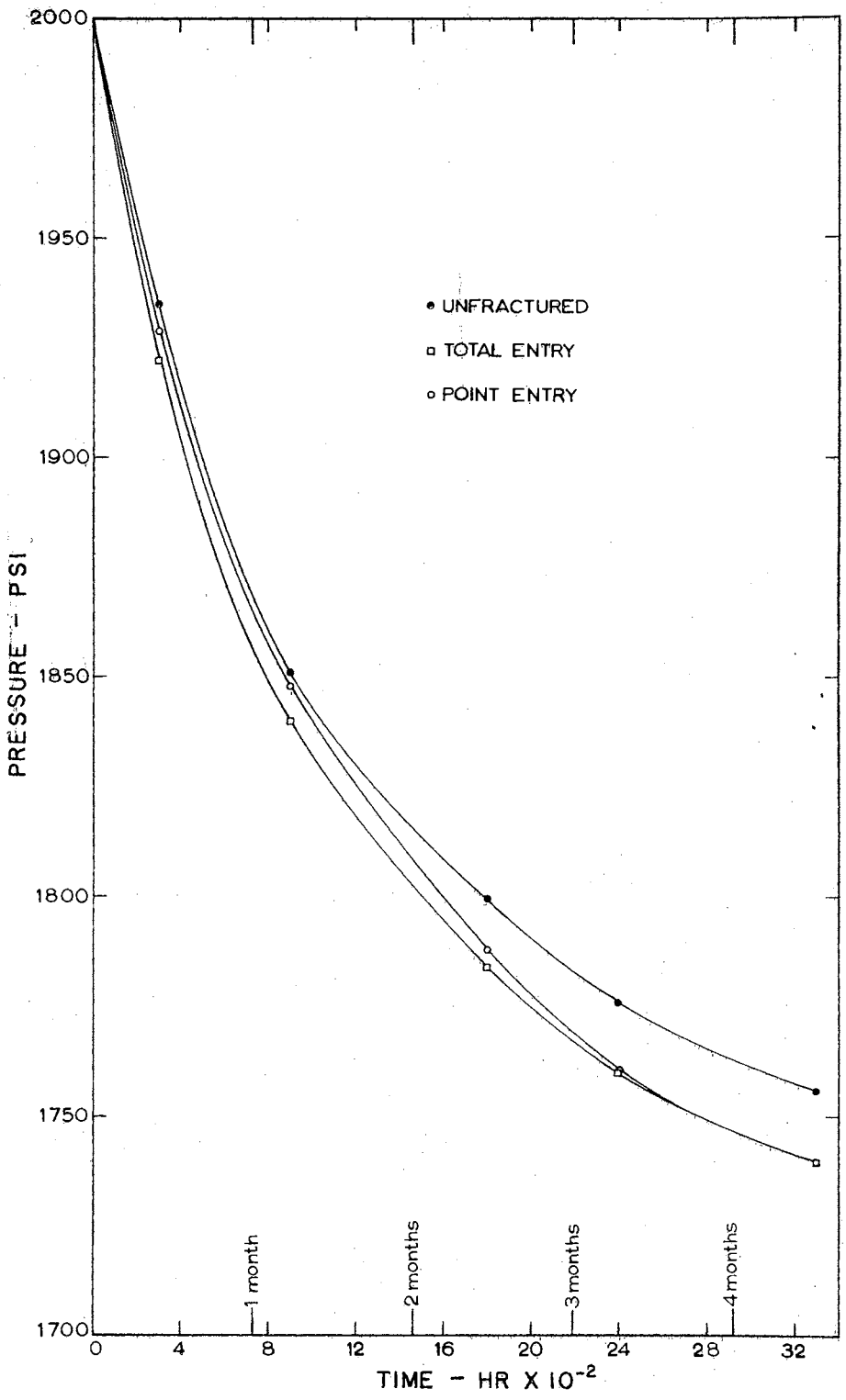

Figure 11. Average Reservoir Pressure Decline Curves.

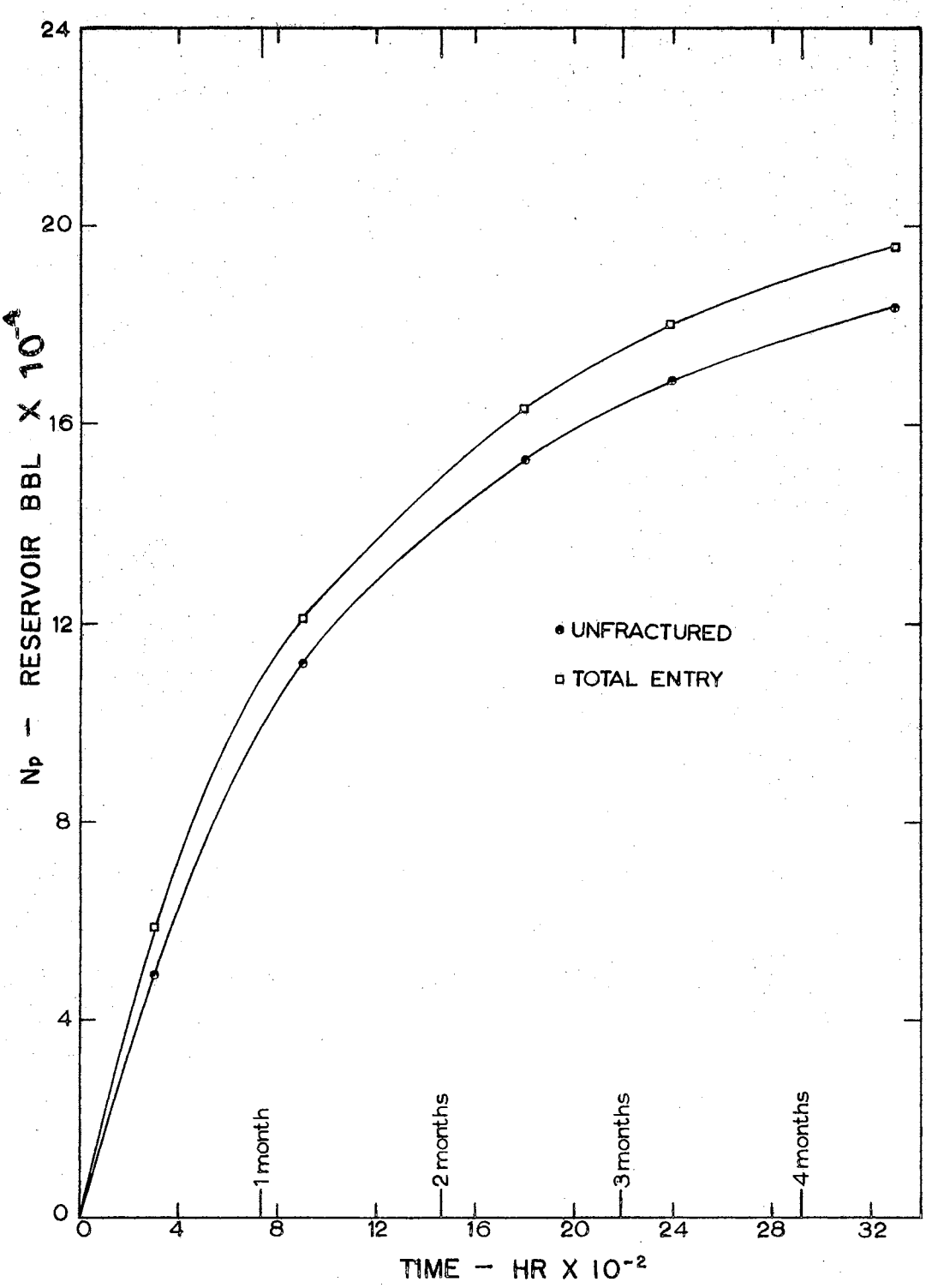

Figure 12. Cumulative Production for the Total-Entry and Un-Fractured Reservoirs.

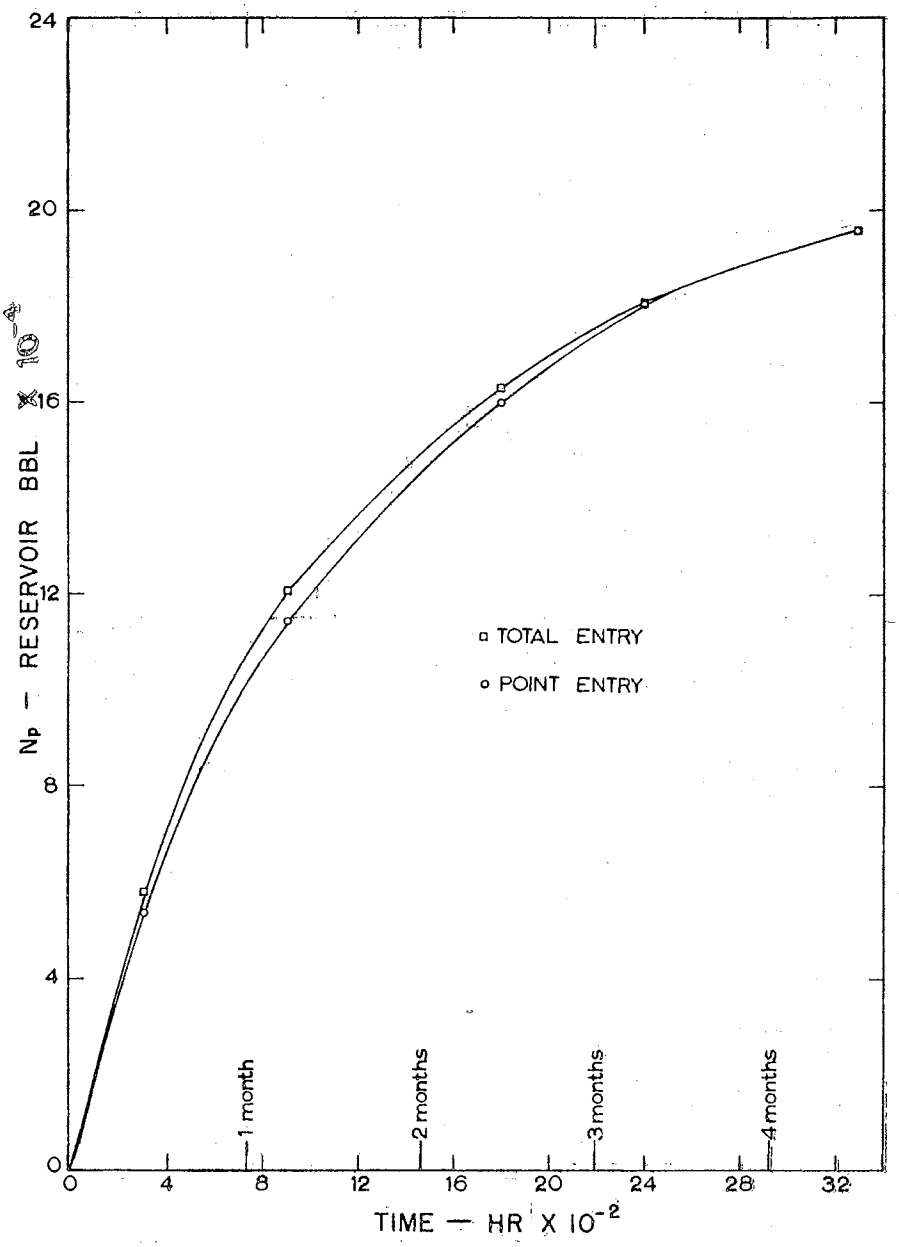

Figure 13. Cumulative Production for the Two Fractured Reservoirs.

behavior difference was attributed to insufficient insulation of the models. The isopotential lines of Figures 9 and 10 show that there was deviation from radial flow, especially near the radial edge of the model. This means that an appreciable amount of thermal energy was passing through the insulation, and that part of the production was actually lost through crossflow. This would present quite a problem in evaluation of an actual reservoir; but for the purpose of this study, which is predominantly comparison, the presence of similar losses in all three models nullified discrepancies caused by these losses.

Exact mathematical descriptions of these reservoirs were abandoned due to deviations from boundary conditions, i.e. losses through insulation, and fluctuation of coolant temperatures. It is felt that the method used in describing the reservoirs is the best available under these circumstances.

CHAPTER VI

CONCLUSIONS

The material derived from this research investigation presented information from which several conclusions may be drawn. It should again be stated that the models used in this research simulated a hypothetical oil reservoir which was producing above the bubble point pressure by liquid expansion drive. The reservoir was also finite in extent, with a closed exterior boundary.

After about 3 1/2 months, the cumulative production of the fractured reservoir with point-entry equaled that of the fractured reservoir with full wellbore entry. Prior to this time, the reservoir with full wellbore entry exceeded the point-entry reservoir by a maximum of 6,000 reservoir barrels. This maximum, which occurred soon after one month of production, may be explained by the fact that after this period of time, a pressure drop of about 40 psi existed between the reservoir and the full-entry wellbore. This allowed a great deal of fluid to flow directly into the well. In addition, fluid was flowing into the well via the fracture. In the point-entry reservoir the only flow into the wellbore was through the fracture, thus the production was smaller. As time progressed, the pressure differential between the wellbore and the adjacent reservoir decreased, and the major portion of flow was through the fracture. At this time, the pressure gradient between the formation and fracture was

higher for the point-entry reservoir than the corresponding pressure gradient of the other fractured reservoir. This condition caused the two reservoirs to eventually equalize in production.

A similar explanation is offered for the production characteristics of the unfractured reservoir. Initially the production of this reservoir almost equaled that of the point-entry reservoir. As the pressure decreased near the unfractured wellbore, the production difference increased until the end of the period of study. At this time the fractured reservoirs exceeded the unfractured one in oil production by approximately 12,000 reservoir barrels.

This model study led to the following conclusions relating to reservoirs of the described type:

1. During early stages of depletion, a fractured well with total wellbore entry will have a higher production than a well with only point-entry.
2. In later stages of depletion, the total-entry and point-entry wells will be approximately equal in production.
3. Both fracture types included in the study will increase the productivity of a reservoir.
4. The assumption of point-entry into a fractured wellbore is a close approximation, even if total wellbore entry exists in the actual reservoir.

CHAPTER VII

RECOMMENDATIONS FOR FUTURE STUDY

One of the most undesirable occurrences during the experimental runs was the flow of heat through the insulation of the models. This resulted in accelerated cooling of the model, and it also caused unexpected deviation from radial flow. Several steps may be taken to reduce the magnitude of this problem. These steps are (a) using thicker insulation, (b) using insulation with a lower thermal conductivity and, (c) using a modeling material with a higher thermal conductivity. The first two steps would increase resistance to heat flow in all directions except toward the wellbore while the third step would allow easier flow of heat through the model to the wellbore.

Reservoir Engineering literature contains a great deal of discussion and mathematics pertaining to oil reservoirs with infinite drainage radii. The assumption of an infinite drainage radius applies to the case where there is flow across the external boundary to replace the fluid produced at the wellbore. This flow across the external boundary results in the maintenance of a constant pressure at the external radius.

The models of this study could be converted to infinite radii models by equipping the exterior radial boundaries with an electrical heating element. The element could have a variable control, and when the temperature at the back of the model began to decline, the element could be adjusted

to maintain the initial temperature at the exterior radial surface.

An important study could be made by placing multiple fractures in a model and comparing the behavior to behaviors of models similar to those used in this investigation. Interesting comparisons might also be obtained by varying the radius of the fracture, or by displacing the fracture from the center of the formation.

As was mentioned eariler, the differences in behavior of the fractured and unfractured reservoirs were not as great as was desired. These differences could be increased by decreasing the model size and increasing the thickness of the fractures. The resulting greater average thermal conductivities of the fractured models would cause the desired greater production increases.

The last recommendation is that the wellbore temperature be held more nearly constant during cooling. The long duration of the runs of this investigation prohibited the use of iced or boiling water as a coolant. A sufficient volume and a constant flow rate of these coolants would have been impossible to acquire over a 20 hour run. Perhaps the use of smaller models with lower initial temperatures would decrease the cooling time and coolant volume requirements, thus permitting the use of one of these constant temperature coolants. Consideration might also be given to the performance of runs in the winter, when diurnal variations are often negligible. Tap water could be used at this time of year with a minimum amount of coolant temperature variation.

SELECTED BIBLIOGRAPHY

1. Hartsock, J. H., and J. E. Warren. "The Effect of Horizontal Hydraulic Fracturing on Well Performance," Journal of Petroleum Technology, Volume 13, No. 10, p. 1050. October, 1961.

2. Van Poolen, H. K. "Do Fracture Fluids Damage Producitivity?" Formation Fracturing, Oil and Gas Journal Technical Manual p. 48. January 4, 1960.

3. Crawford, Paul B., and Bobby L. Landrum. "Estimated Effect of Horizontal Fractures on Production Capacity," Paper No. 414-G, Fall Meeting of Petroleum Branch of AIME, October, 1954.

4. Pickering, Charles H., N. T. Cotman, and Paul B. Crawford, "A Study of Flow in Stratified Reservoirs by Use of the Thermal Analogy," Society of Petroleum Engineers Journal, p. 215. December, 1961.

5. Landrum, Bobby L., Donald A. Flanagan, Billy C. Norwood, and Paul B. Crawford. "A New Experimental Model for Studying Transient Phenomena," AIME Volume 216, p. 33. 1959.

6. Schneider, P. J. Conduction Heat Transfer. Addison-Wesley Publishing Co., Mass, p. 3. 1957.

7. Collins, R. E. Flow of Fluids Through Porous Materials. Reinhold Publishing Corp., New York, p. 71. 1961.

APPENDIX A

CORRELATION BETWEEN FLUID FLOW AND HEAT CONDUCTION

Fourier's conduction law states that the flux of heat conducted across a surface is proportional to the temperature gradient taken in a direction normal to the surface of the point in question. Beginning with this basic law, an energy balance can be made on an infinitesimal solid element such as shown in Figure 14. Considering only conduction in the x-direction:

$$q_{in} = - \left(K_x \frac{\partial T}{\partial x} \right)_x dydz \tag{A-1}$$

$$q_{out} = - \left(K_x \frac{\partial T}{\partial x} \right)_{x+dx} dydz \tag{A-2}$$

Expanding q_{out} in a Taylor's series and neglecting all terms after the first two:

$$- \left(K_x \frac{\partial T}{\partial x} \right)_{x+dx} dydz = - \left(K_x \frac{\partial T}{\partial x} \right)_x dydz + \frac{\partial}{\partial x} \left[\left(- K_x \frac{\partial T}{\partial x} \right)_x dydz \right] dx \tag{A-3}$$

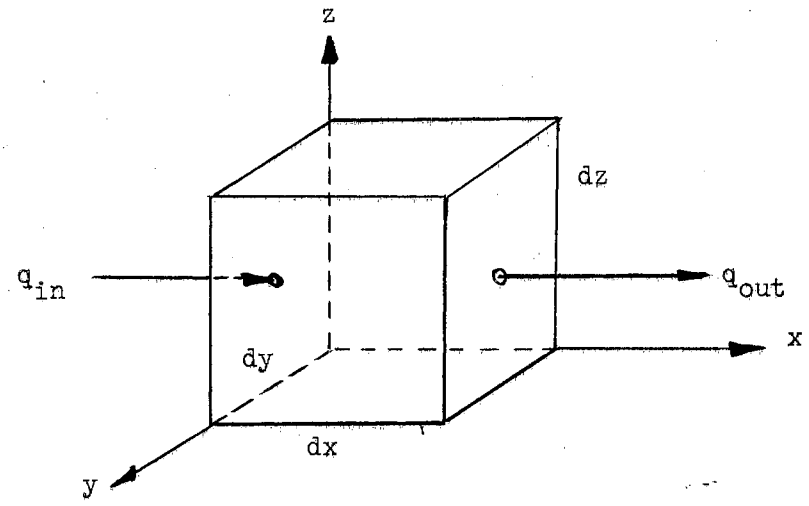

Figure 14. Heat Conduction Through a Differential Element.

The change of q over the distance dx is given by $q_{in} - q_{out}$:

$$(\Delta q)_x = -\left(K_x \frac{\partial T}{\partial x}\right)_x dydz - \left\{ -\left(K_x \frac{\partial T}{\partial x}\right)_x dydz + \frac{\partial}{\partial x}\left[\left(-K_x \frac{\partial T}{\partial x}\right)_x dydz\right] dx \right\} =$$

$$\frac{\partial}{\partial x}\left(K_x \frac{\partial T}{\partial x}\right) dydzdx \qquad \text{(A-4)}$$

Using similar reasoning for the other axes:

$$(\Delta q)_y = \frac{\partial}{\partial y}\left(K_y \frac{\partial T}{\partial y}\right) dxdzdy \qquad \text{(A-5)}$$

$$(\Delta q)_z = \frac{\partial}{\partial z}\left(K_z \frac{\partial T}{\partial z}\right) dxdydz \qquad \text{(A-6)}$$

The sum of these Δq's gives the total rate of heat storage in the element as:

$$dxdydz \left[\frac{\partial}{\partial x}\left(K_x \frac{\partial T}{\partial x}\right) + \frac{\partial}{\partial y}\left(K_y \frac{\partial T}{\partial y}\right) + \frac{\partial}{\partial z}\left(K_z \frac{\partial T}{\partial z}\right) \right] \qquad \text{(A-7)}$$

The total rate of heat storage in the element may also be expressed by:

$$\rho C \frac{dT}{dt} dxdydz \qquad \text{(A-8)}$$

where

$$\frac{dT}{dt} = \frac{\partial T}{\partial t} + \frac{\partial T}{\partial x}\frac{dx}{dt} + \frac{\partial T}{\partial y}\frac{dy}{dt} + \frac{\partial T}{\partial z}\frac{dz}{dt} \qquad \text{(A-9)}$$

Since $\frac{dx}{dt} = \frac{dy}{dt} = \frac{dz}{dt} = 0$ for a mass at rest,

then,

$$\frac{dT}{dt} = \frac{\partial T}{\partial t} . \qquad \text{(A-10)}$$

Making the assumptions that there is no internal heat generation, and that K, and C are constant; then setting the expressions for rate of heat storage equal and simplifying:

$$\rho C \frac{\partial T}{\partial t} = K\left(\frac{\partial^2 T}{\partial x^2} + \frac{\partial^2 T}{\partial y^2} + \frac{\partial^2 T}{\partial z^2}\right) \qquad \text{(A-11)}$$

Using the LaPlacian operator ∇^2 and letting $\alpha = \frac{K}{\rho C}$ = thermal diffusivity, yields:

$$\nabla^2 T = \frac{1}{\alpha}\frac{\partial T}{\partial t} \qquad \text{(A-12)}$$

The above derivation is similar to that of Schneider (6).

A similar equation may be obtained for fluid flow. Collins (7) states that in the flow of a compressible fluid through a porous medium, the mass of an element of the fluid remains constant even though pressure fluctuation causes a change in volume. For this type of flow, the equation of continuity may appear as:

$$- \nabla \cdot (\rho u) = \frac{\partial(\Phi\rho)}{\partial t} \tag{A-13}$$

In the case of an isotropic porous medium with negligible gravitational effects, Darcy's law becomes:

$$u = - \frac{k}{\mu} \nabla P \tag{A-14}$$

Substituting this into the continuity equation yields

$$\nabla \cdot \left(\frac{k\rho}{\mu} \nabla P \right) = \Phi \frac{\partial \rho}{\partial t} \tag{A-15}$$

For an ideal liquid

$$c = \frac{1}{\rho} \frac{d\rho}{dP} = \text{constant} \tag{A-16}$$

therefore

$$\rho \nabla P = \frac{1}{c} \nabla \rho \tag{A-17}$$

Thus, if c is considered constant, the differential equation for the flow of an ideal compressible liquid through an isotropic, incompressible, homogeneous medium is, for negligible gravitational effects

$$\nabla^2 \rho = \frac{\Phi \mu c}{k} \frac{\partial \rho}{\partial t} \tag{A-18}$$

The equation of state for a slightly compressible liquid may be written as

$$\rho = \rho_o e^{c(p-p_o)} = \rho_o \left[1+c(p-p_o)+ 1/2!\ c^2(p-p_o)^2 + \cdots\right] \qquad \text{(A-19)}$$

Finding $\nabla^2\rho$ from this equation and ignoring both the terms greater than c^2 and the squares of partial derivatives:

$$\nabla^2\rho = (c\rho_o+c^2\rho_o p-c^2\rho_o p_o)\left(\frac{\partial^2 p}{\partial x^2}+\frac{\partial^2 p}{\partial y^2}+\frac{\partial^2 p}{\partial z^2}\right) \qquad \text{(A-20)}$$

also

$$\frac{\partial \rho}{\partial t} = \frac{\partial p}{\partial t}\ (c\rho_o+c^2 p\rho_o-c^2\rho_o p_o) \qquad \text{(A-21)}$$

Substituting these into Equation (A-18) and simplifying yields

$$\frac{\partial^2 p}{\partial x^2} + \frac{\partial^2 p}{\partial y^2} + \frac{\partial^2 p}{\partial z^2} = \frac{\phi\mu c}{k}\ \frac{\partial p}{\partial t} \qquad \text{(A-22)}$$

or

$$\nabla^2 p = \frac{\phi\mu c}{k}\ \frac{\partial p}{\partial t} \qquad \text{(A-23)}$$

It is apparent that Equations (A-12) and (A-23) are similar. In order to make them comparable, certain dimensionless groups (5) must be introduced. Using the subscripts m and r to denote heat and fluid, respectively, dimensionless times may be given by

$$(t_D)_m = \frac{\alpha t_m}{L_m^2}, \qquad (t_D)_r = \frac{k\ t_r}{\phi c\mu L_r^2} \qquad \text{(A-24)}$$

Other dimensionless groups are

$$\frac{P_i - P}{P_i - P_w} = P_D, \qquad \frac{T_i - T}{T_i - T_w} = T_D$$

$$\frac{X}{L_r} = X_D, \qquad \frac{Y}{L_r} = Y_D, \qquad \frac{Z}{L_r} = Z_D \tag{A-25}$$

$$\frac{x}{L_m} = x_D, \qquad \frac{y}{L_m} = y_D, \qquad \frac{z}{L_m} = z_D$$

Equations (A-12) and (A-23) may now be written as Equations (A-26) and (A-27).

$$\nabla^2 p = \frac{\partial PD}{\partial (t_D)_r} \tag{A-26}$$

$$\nabla^2 T = \frac{\partial T_D}{\partial (t_D)_m} \tag{A-27}$$

Heat and fluid flow phenomena may be related by setting $t_{Dm} = t_{Dr}$, resulting in

$$\frac{\alpha t_m}{L_m^2} = \frac{k t_r}{\Phi c \mu L_r^2} \tag{A-28}$$

APPENDIX B

LIST OF SYMBOLS

A	Area, in^2
A_j	Planimetered value of j^{th} area, in^2
B_o	Formation volume factor, reservoir bbl/STB
c	Liquid compressibility, psi^{-1}
C	Specific heat, Btu/lb^{o} F
e	Natural logarithm base
h	Formation thickness, ft
h_r	Hypothetical reservoir formation thickness, ft
k	Absolute permeability, md
K	Thermal conductivity, $Btu \cdot in/hr \cdot ft^2 \cdot {}^{o}F$
$(kh)_r$	Radial flow capacity of formation, md-ft
L_m	Model reservoir radius, ft
L_r	Hypothetical reservoir radius, ft
m	Slope of linear portion of pressure build-up curve, psi/cycle
N_p	Cumulative production, reservoir bbl
P	Reservoir pressure, psi
P_{avg}	Average reservoir pressure, psi
P_D	Dimensionless pressure
P_i	Initial reservoir pressure, psi

P_j	Average pressure of j^{th} area, psi
P_o	Base pressure, psi
P_w	Wellbore pressure, psi
P_{wi}	Built-up pressure one hour after shut-in, psi
P_{wo}	Flowing wellbore pressure at shut-in, psi
$(PI)_r$	Stabilized productivity index before fracturing, STB/day/psi
$(PI)_f$	Stabilized productivity index after fracturing, STB/day/psi
ΔP	Pressure drop, psi
$(\Delta P)_f$	Pressure drawdown of fractured system, psi
$(\Delta P)_r$	Pressure drawdown of unfractured system, psi
q	Oil production rate, STB/day
q_f	Production rate of fractured system, STB/day
q_{in}	Heat flux into element, Btu/hr
q_{out}	Heat flux out of element, Btu/hr
q_r	Production rate of unfractured system, STB/day
Δq	Change in heat flux, Btu/hr
r_e	Drainage radius, ft
r_w	Wellbore radius, ft
S	Apparent skin effect, dimensionless
t	Time, hr
T	Temperature, ^oF
T_D	Dimensionless temperature
$(t_D)_m$	Dimensionless model time
$(t_D)_r$	Dimensionless reservoir time

T_i	Initial temperature, ^oF
t_m	Model time, hr
t_r	Reservoir time, hr
T_w	Wellbore temperature, ^oF
Δt	Change in time, hr
u	Fluid velocity, ft/sec
V	Volume of liquid, reservoir bbl
x, y, z	Cartesian coordinate position variables
x, y, z	Position variables for hypothetical reservoir, Equation (A-25)
X, Y, Z	Position variables for models
x_d, y_d, z_d	Dimensionless position variables for hypothetical reservoir
X_D, Y_D, Z_D	Dimensionless position variables for models
α	Alpha, thermal diffusivity, cm^2/sec
Φ	Phi, porosity, dimensionless
∇	Del operator
∇^2	LaPlacian operator
μ	Mu, viscosity of liquid, cp
θ	Thetha, sector angle, degrees
ρ	Rho, density, lb/ft^3
ρ_o	Base density, lb/ft^3

VITA

James Robert Clark

Candidate for the Degree of

Master of Science

Thesis: A THERMAL MODEL STUDY OF A HYPOTHETICAL FRACTURED OIL RESERVOIR

Major Field: Mechanical Engineering

Biographical:

Personal Data: Born September 21, 1939, in Wilson, Oklahoma, the son of Norman and Irene Clark.

Education: Graduated from Wilson High School, Wilson, Oklahoma, in 1957; received the Bachelor of Science degree from Oklahoma State University, with a major in Mechanical Engineering, in May, 1962; completed the requirements for the Master of Science degree in September, 1963.

Experience: Employed as a part-time Research Assistant in the School of Mechanical Engineering, Oklahoma State University, from June, 1963 to September, 1963.

Honorary Organizations: Pi Tau Sigma, Sigma Tau.

Honors and Awards: Who's Who Among Students in American Universities and Colleges, 1961-1962. Awarded Pan American Fellowship in Mechanical Engineering 1962-1963.